ChemComm

Time-Resolved Radioluminescence of the Cu(I) Cluster $Cu_4I_6^{2-}$. Different Responses to Photo, X-Ray, β-Ray and α-Particle Excitation

Journal:	*ChemComm*
Manuscript ID	CC-COM-10-2023-004870.R1
Article Type:	Communication

COMMUNICATION

Time-Resolved Radioluminescence of the Cu(I) Cluster $Cu_4I_6^{2-}$. Different Responses to Photo, X-Ray, β-Ray and α-Particle Excitation

Received 00th January 20xx,
Accepted 00th January 20xx

DOI: 10.1039/x0xx00000x

John V. Garcia,[a,#] Camilo Guzman,[a,#] Alexander A. Mikhailovsky,[a] Sean Devitt,[a] James R. Tinsley,[b,*] John A. DiBenedetto [b,*] and Peter C. Ford [a,*]

Time-resolved radioluminescence (TRRL) properties of the Cu(I) cluster $Cu_4I_6^{2-}$ upon pulsed X-ray, β-ray or α-particle excitation are described. The longer (>2 μs) TRRL component display exponential decay comparable to pulsed UV excitation; however, temporal behavior at shorter times indicates that high local excited state density provides an alternative decay channel.

Radioluminescence (RL) is a sought-after materials property in development of radiation detectors and imagers for homeland security, medicine, etc.[1] In this regard, metal complexes have drawn considerable attention, as they can be incorporated into inorganic and organic matrices or developed into nanocarriers. Among these, there has been a growing interest in RL from copper(I) iodide clusters[2-7] given the strong, environmental-sensitive photoluminescence (PL) of these assemblies.[8-13] Recent studies identified several multinuclear Cu(I) complexes as scintillators when subjected to X-ray radiation including the clusters $Cu_4I_4L_4$ (L = pyridine or PPh_3)[2] and salts of $Cu_4I_6^{2-}$, several of which have been fabricated into devices for radiation detection and imaging.[6,7] Here, we examine, for the first time, time-resolved radioluminescence (TRRL) properties of two $Cu_4I_6^{2-}$ salts, $[Na_2(18\text{-crown-}6)_2(H_2O)_3][Cu_4I_6]$ (**I**) and $[Li(benzo\text{-}15\text{-crown-}5)_2(H_2O)]_2[Cu_4I_6]$ (**II**). Temporal responses of scintillation when the excitation sources are X-rays, β-rays or α-particles differ from the time-resolved photoluminescence (TRPL) of **I** and **II** upon UV excitation and also from each other. The common theme is that photophysical behaviour is determined by the $Cu_4I_6^{2-}$ anion with the corresponding cation having relatively little effect. However, the mode of excitation does make a marked difference in the temporal responses.

Slow evaporation of the solution used to prepare **I** (Supporting Information: Experimental Methods) gave crystalline plates and square blocks while similar preparation of **II** gave crystalline yellow platelets (Fig. 1). Both materials showed intense luminescence under 365 nm irradiation. The crystal structures of **I** and **II** have been reported,[14] and the redetermined structure of the synthesized **II** reproduced the published structure. These show the $Cu_4I_6^{2-}$ unit as an octahedron of six iodide ions encapsulating four copper(I) ions with 50% occupancy of 8 equivalent copper sites owing to the two equivalent orientations for the Cu_4 tetrahedra (Fig. 1c). The $Cu_4I_6^{2-}$ clusters are sufficiently separated in the crystal to be considered discrete chromophores.

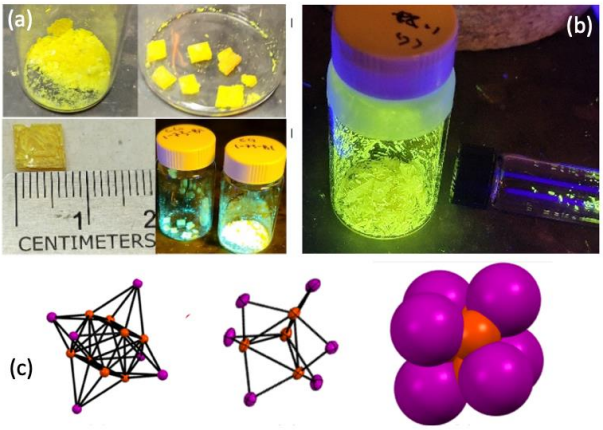

Figure 1. **(a)** **I** under ambient light and under a black light. **(b)** Crystalline **II** under the black light. **(c)** Representations of $Cu_4I_6^{2-}$ anion in **I** (and **II**) showing disorder of Cu_4 centre in crystal structure (left), one tetrahedral arrangement of Cu_4 centre (middle), space-filling representation (right)

The PL spectrum of solid **I** recorded using a PTI fluorimeter displayed a λ_{max}^{em} at 535 nm when excited at 450 nm (SI Fig S1) while the excitation spectrum (monitored at 535 nm) showed a broad excitation band from ~275 to 500 nm, qualitatively similar to the diffuse reflectance spectrum (SI Figs. S2 & S3). The PL spectrum of **II** was identical (λ_{max}^{em} 535 nm (SI Fig. S4), as reported for other $Cu_4I_6^{2-}$ salts.[6b,15,16] The band position and shape are independent of the counter ion, consistent with this cluster being essentially isostructural in these solids and the only luminescent chromophore.

The TRPL of solid **I** recorded at ambient temperature using pulsed laser excitation gave *strictly exponential* PL decay (Fig. 2a). The measured lifetime τ_{PL} was 2.16 μs. Overall, the photophysical properties described here for **I** closely parallel those reported by Huang et al.,[15] who determined a τ_{PL} of 2.14 μs and a PL quantum yield of 0.92 for excitation (λ_{ex}) at 450 nm. The TRPL of ambient **II** also gave strictly exponential decays with τ_{PL} values of 2.54 μs (λ_{ex} 270) and 2.79 μs (λ_{ex} 450 nm) (SI Fig. S5).

[a] *Department of Chemistry and Biochemistry, University of California, Santa Barbara, Santa Barbara, CA, 93106-9510 USA.*
[b] *Special Technologies Laboratory, 5520 Ekwill Street, Suite B, Santa Barbara, CA 93117*
*Corresponding DibeneJA@nv.doe.gov, **TINSLEJR@nv.doe.gov**, pcford@ucsb.edu
# these authosr contributed equally
Electronic supplementary information (ESI) available: Materials,, experimental procedures, one scheme and 16 figures (15 pages total, PDF).
See DOI: 10.1039/x0xx00000x

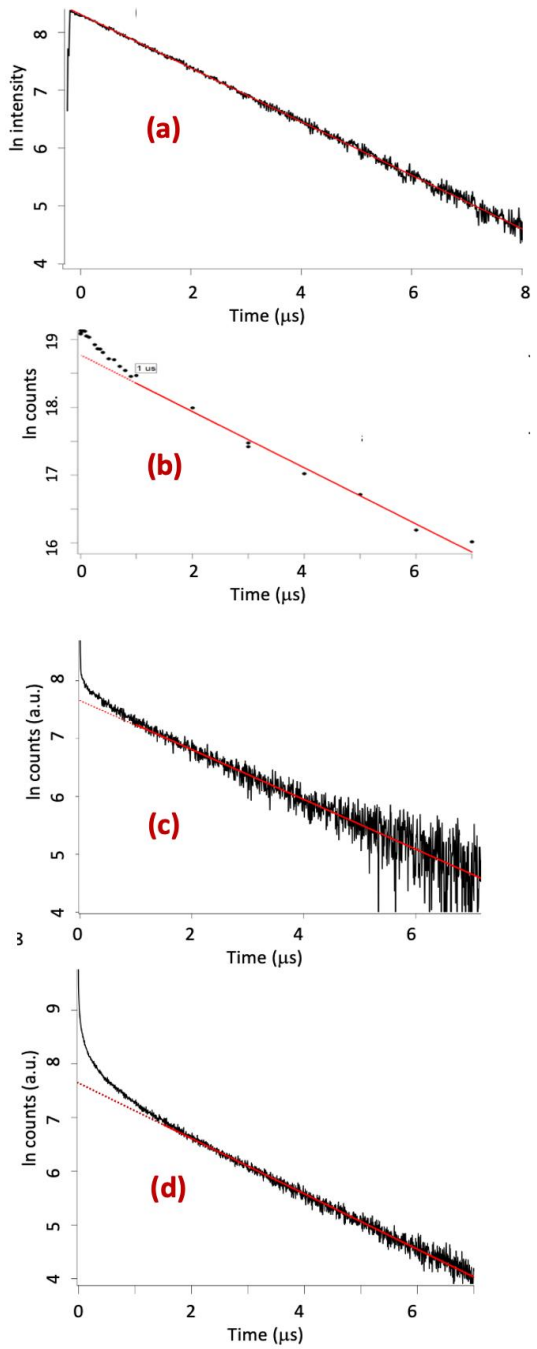

Figure 2. (a) PL decay of crystalline **I** upon pulsed laser excitation at 370 nm monitored at 535 nm with data points collected at 10 ns intervals showing single exponential decay with τ_{PL} = 2.16 μs. **(b)** Log plot of the integrated RL intensity as a function of the time delay from pulsed X-ray excitation (150 keV) of **I**. The solid red line is the linear fit of these data from 1 μs to 7 μs. The slope ($-k_d$) is –0.415 μs^{-1}; $\tau_{RL} = 1/k_d$ = 2.41 μs. **(c).** Ln(counts) plot vs time of the scintillation data from **I** using the Fluor Decay System (FDS, see SI: Experimental methods) with β-particle excitation from a ^{90}Sr source and single photon counting with 6.1 ns resolution. τ_{RL} = 2.32 μs for the time frame 1-7.7 μs. **(d)** Ln(counts) plot vs time of the scintillation data from crystalline **I** using the FDS with 4.9 ns resolution and α-particle excitation from a ^{244}Cm source. τ_{RL} = 1.93 μs for the time frame 1.5-7.0 μs. For **(b)**, **(c)** and **(d),** the red dotted line is the linear extension of the ln(counts) plots at longer time frames (red lines) to emphasize the marked departure from single exponential decay in the early stages of TRRL decay.

Time dependent density functional theory (TDDFT) studies[17] for the $Cu_4I_6^{2-}$ chromophore of $(PPh_4)_2[Cu_4I_6]\cdot 2(CH_3)_2CO$ attributed the emission to an excited state (ES) having intermetallic bonding character in the Cu_4 cube and substantial distortion from the ground state structure. These conclusions parallel earlier *ab-initio*[18] and TDDFT computations[19] of $Cu_4I_4py_4$ assigning the lowest ES as a "cluster-centered" triplet state ($^3CC^*$) delocalized over the Cu_4I_4 chromophore. The PL lifetimes exceeding 2 μs for ambient **I** and **II** are consistent with an ES of "triplet" character.

The integrated RL spectrum of **I** measured with continuous X-ray excitation (40 kV, 30 mA) proved to be essentially identical to the PL spectrum (SI Fig. S1). The coincidence of the PL and RL spectra for **I** was also recently described by Wang et al[6a] and analogous observations have been made for other $Cu_4I_6^{2-}$ salts including **II** (see below).

The TRRL behaviours of crystalline **I** and **II** were examined by using pulsed X-ray excitation (2.5 mRad, 40 ns pulses at ~25 Hz) (SI: Experimental Methods) at the Special Technologies Laboratory (STL). The TRRL spectra were recorded for specific time windows using either a 50 ns or a 1 μs gate-width set with different time delays. The integrated intensities of these gated spectra were also used to evaluate the decay rates of the resulting RL.

Notably, the TRRL decay from the pulsed X-ray excitation (Fig. 2b) *shows a distinct departure from exponential behaviour* at the shortest delay times. For **I**, the plot of ln(counts) ("counts" being the integrated RL intensity for the time resolved spectrum) versus time was linear over the 1 to 7 μs time period. The resulting measured RL lifetime (2.41 μs) is close to the PL lifetime (2.16 μs). However, at observation times < 1 μs, the plot curves upward indicating that the emission is decaying faster before levelling to give behaviour comparable to the TRPL. Analogous non-exponential decay is also evident for X-ray excitation of **II** (SI Fig. S6).

Given that these X-ray photons are >3 orders of magnitude higher energy than the UV photons used in PL experiments, several scenarios may be responsible. X-rays interact with high cross-section atoms to ionize inner-shell electrons (photoelectric effect) to produce secondary electrons that generate multiple free excitons, then the ES or self-trapped excitons (STE) responsible for scintillation. The initial high energy processes are very fast (10^{-15}-10^{-13} s), while the localization at luminescent centres is slower (10^{-12}-10^{-8} s).[20] Since X-ray photon interactions with crystalline solids access very high energy states and/or excitons not accessible upon absorption of a UV photon, the non-exponential behaviour might reflect emission from such states. Another consequence of X-ray excitation is the deposition of much more energy in a confined space than likely with UV photons, thereby generating multiple ES (STEs) in close proximity. The coupling of these with each other provides a mechanism (ES/ES annihilation) toward faster decay.[21] Once localized ES concentrations diminish, the dominant pathway would be unimolecular decay comparable to the PL experiment.

The first alternative should be reflected in the RL spectra; however, within experimental uncertainty, the TRRL spectra recorded at the earliest time delays and smallest gate widths (50 ns) are identical to those measured at longer delays (Fig. 3, SI Fig. S7). The shape and ν_{max} of the emission spectra are consistent for all delay times, even the shortest, after X-ray excitation. Thus, TRRL from **I** occurs from the same $Cu_4I_6^{2-}$ state(s) over the entire-time frame of observation. Absorption of X-rays generate the CC* state(s) responsible for RL

(and for PL) within 50 ns, and the RL spectra reflect the emission from this common ES. Analogous TRRL experiments with **II** gave the same temporal spectra (SI Fig. S8), confirming that the key chromophore is the $Cu_4I_6^{2-}$ cluster. The strictly exponential PL decays imply internal conversion/intersystem crossing (IC/ISC) to the emissive states on a much faster time frame, consistent with sub-ns IC/ISC rates found with other metal complexes.[22]

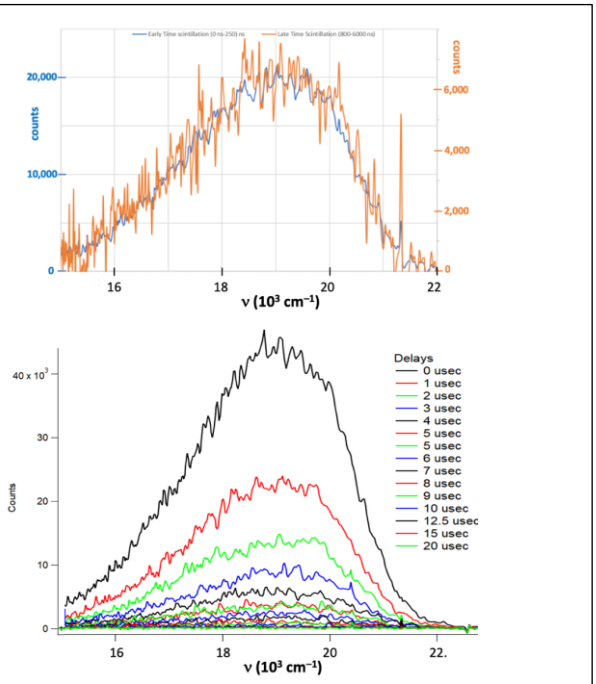

Figure 3. Temporal RL spectra of solid **I:** *Bottom:* Recorded using a 1 μs gate (time window) with time delays of 1 μs intervals after pulsed X-ray excitation. The first spectrum was measured with no delay. *Top:* The short time spectrum (blue curve) shows the integrated sum of individual traces captured at time windows of 50 ns and time delays from 0 to 250 ns. The second trace (orange curve) sums the spectra recorded with 50 ns time windows at time delays from 800 to 6000 ns. The coincidence of the spectra captured very soon after excitation and much later indicate that the same ES is responsible for the scintillation throughout the observa-

Concern that the non-linearity of the TRRL decays noted in Figures 2b and S6 may represent an unanticipated artifact led us to explore high energy radiation excitation with different instrumentation. In this application, the Fluor Decay System (FDS) at STL (SI: Experimental Methods)[23] used β-rays (≤ 546 keV) emitted from a ^{90}Sr source for excitation and single photon counting with 6.1 ns resolution to record the time dependence of the resulting scintillation (Fig. 2c). At t >1 μs, the plot of ln(counts) (where "counts" are proportional to intensity) were linear and gave lifetime of 2.32 μs, very close to those recorded for TRPL and for TRRL using X-ray excitation. However, in agreement with the X-ray experiment, the early RL decay from β-ray excitation departs from the exponential fit and distinctly displays a faster component. This behaviour is duplicated for the analogous β-ray excitation of **II** (SI Fig. S9) where the longer component of the decay gave a τ_{RL} of 2.53 μs. These results substantiate that the non-exponential TRRL decay observed in Figs. 2b, 2c, S6 and S9 (in contrast to the strictly linear PL decay) results from excitation with the much higher energy X- and β-rays.

The premise that the non-exponential TRRL decays seen upon X- or β-ray excitation of **I** and **II** are due to high ES (STE) densities formed at the interaction site stimulated the following α-particle excitation experiment. The higher energies and greater cross-sections of α-particles should generate even higher ES densities at the impact site and a more emphatic departure from unimolecular decay. This prediction was emphatically confirmed.

TRRL triggered by α-particles was recorded using the FDS equipped with a ^{244}Cm source, which emits 5.763 MeV and 5.806 MeV α-particles. The source has a stainless-steel foil window designed to allow α-particles to escape, but with attenuated energy (3–3.5 MeV est.). Figures 2d and S10 display the temporal scintillation decays from **I** and **II**, respectively, after α-particle excitation. While, these data demonstrate simple exponential decay after ~1.5 μs with τ_{RL} = 1.93 μs, at a shorter time-frame, the non-exponential component is dramatically more pronounced than with either X-ray or β-ray excitation. The difference between the t = 0 intercept for the normal exponential decay and the observed emission intensity at t = 0 (Figs. 2d & S10) indicates that this alternative pathway accounts for at least 75% of the ES deactivation after α-particle excitation. This component is considerably smaller with X-ray and β-ray excitation.

A recent report by Hundyadi et al.[24] describes using 5.5 MeV α-particles to excite a thin perovskite film scintillator. These workers also noted an early non-exponential decay of the resulting emission and attributed that behaviour to "excitation density-dependent self-trapped exciton recombination". Triplet-triplet annihilation has long been known for organic scintillators,[21] where ES lifetimes are longer and determined by that of the triplet.

When one examines the TRRL from crystalline **I** or **II**, several features are immediately apparent. The first is that upon X-ray excitation, the RL spectra duplicate the PL spectra at all observation times, even during the first few hundred ns. We therefore conclude that this emission is occurring from the same excited state(s) in each case, presumably a CC* triplet localized on the $Cu_4I_6^{2-}$ chromophore. For t > ~1.5 μs, TRRL decay for each excitation mode follows exponential kinetics that parallel the strictly exponential TRPL decays recorded with UV excitation. However, in the shorter time regimes, the TRRL profiles display a fast decay component not seen with TRPL. Furthermore, the magnitude of the fast decay component increases with the energy of the excitation radiation, i.e., X-rays < β-ray s<< α-particles, each being many orders of magnitude more energetic than UV photons and sufficient to generate multiple excitons, hence, multiple luminescent excited states in a relatively small volume of the solid. Therefore, we attribute the unusual decay pattern at the initial TRRL stages to interactions between multiple ES generated in close proximity, since, after several μs, the RL settles into behaviour similar to that of the PL experiments.

Modelling the TRRL pattern where there is both unimolecular and bimolecular decay pathways in the solid is challenging, as also found for long lived triplet-triplet annihilation/upconversion in organic scintillator solids.[25] Given sub-ns IC/ISC, the PL is largely from the lowest energy ES and as observed for the RL of **I** and **II** for which emissive CC* states are, on the time frame of the TRRL experiment, formed immediately. Thus, we attribute the enhanced decay rate in the early stages to interactions between multiple CC* states generated in close proximity upon depositing high energy in a relatively confined volume in the crystal. The rate law might be represented by eq. 1, *if these were dynamic systems with the diffusion properties of a solution, and if the initial ES were generated with a relatively homogeneous distribution*. The k_d values can be derived from linear

parts of Figure 2, etc. ($k_d = \tau^{-1}$). However, it was not surprising that attempts to fit the TRRL decays to the resulting differential equation (SI Scheme S1) were unconvincing. Eq. 1 does not take into account a mechanism where there would be multiple CC* at varied, but fixed, distances from each other in the solid. As a result, k_q is not a constant but would depend (exponentially) on the distance between respective ES (assuming the Dexter mechanism for energy transfer). Another potential complication would be exciton migration within the crystal, if such migration occurs on a relevant time scale. Lastly, the distribution of the multiple excited molecules resulting from the interaction of the high energy particles with these cuprous crystals will not be homogenous. Thus, Monte Carlo simulation may be the best approach to modelling the temporal RL; however, such analysis is outside the scope of this communication.

$$-d[CC^*]/dt = k_d[CC^*] + k_q[CC^*]^2 \quad (1)$$

SI Figures S11-S13 display double exponential fits of the early stage (30 ns to 3 μs) TRRL data for **I** and **II**. In treating these data, k_d was held constant at the value determined over the 2 to 7 μs time frame. While the fits for the X-ray and β-ray experiments were qualitatively convincing, those for α–particle excitations were much less so. What this treatment does provide is further confirmation of the much greater magnitude of the early decay component for the latter experiments. Regardless, it is unclear what would be the physical significance of such double exponential analysis.

In summary, earlier PL studies have shown that compounds containing the anionic cluster $Cu_4I_6^{2-}$ are strongly luminescent with very high quantum yields[16] and that polymer composites with **I** can be fabricated into devices with very sensitive X-ray detection limits.[6] The TRRL studies described here add new insight into the scintillator properties of this interesting chromophore. While the RL spectrum of $Cu_4I_6^{2-}$ under continuous excitation duplicates the PL spectrum, it is particularly relevant that the same spectrum is observed under pulsed X-ray excitation. Thus, within the time resolution of these experiments (<50 ns), the emitting excited state(s) generated by X-ray excitation is the same as that also generated by photoexcitation. At longer observation times (>1 μs), this point is emphasized by the near coincidence of the RL and PL lifetimes determined from the linear exponential plots. However, while PL decays follow the strictly exponential behaviour at shorter observation times, RL decays deviate markedly and demonstrating a much faster component. Furthermore, this component is increasingly prominent with excitation by β-rays and (more so) by α–particles. We conclude that the latter behaviour can be attributed to biomolecular self-quenching owing to the localized density of excited states (self-trapped excitons) generated by high energy radiation. That density will be a factor both of the energy and of the absorption cross-section of the exciting radiation with the specific material under study. These features offer a potential for differentiating radiation types with such materials.

This project was supported by Mission Support and Test Services, LLC under Contract No DENA0003624 with the U.S. Department of Energy, supported by the Site-Directed Research and Development Program DOE/NV/03624-1237 and the UCSB Academic Senate. UCSB time-resolved spectroscopy instrumentation was supported by DoD ARO DURIP award 66886LSRIP.

Conflicts of interest

There are no conflicts to declare.

Notes and references

1. (a) C. Dujardin, E. Auffray, E. Bourret-Courchesne, P. Dorenbos, P. Lecoq, M. Nikl, A. N.Vasil'ev, A. Yoshikawa, R.-Y. Zhu, *IEEE Trans. Nuc. Sci.* 2018, **65**, 1977.
2. K. Kirakci, K. Fejfarová, J. Martinčík, M. Nikl, K. Lang, *Inorg. Chem*. 2017, **56**, 4609.
3. S.-Y. Yin, Z. Wang, Z.-M. Liu, H.-J. Yu, J.-H. Zhang, Y. Wang, R. Mao, M. Pan, C.-Y. Su, *Inorg. Chem*. 2019**, 58**, 10736.
4. N. Zhang, L. Qu, S. Dai, G. Xie, G. Zhang, C. Han, R. Huo, H. Hu, Q. Chen, W. Huang, H. Xu, *Nature Commun.*, 2023, 14, 2901.
5. Q. Zhou, J. Ren, J. Xiao, L. Lei, F. Liao, H. Di, C. Wang, L. Yang, L., X. Yang, Y. Zhao, X. Han, *Nanoscale*, 2021, **13**, 19894.
6. (a) H. Wang, J.-X. Wang, X. Song, T. He, Y. Zhou, O. Shekhah, L. Gutirrez-Arzaluz, M. Bayindir, M. Eddaoudi, O. M. Bakr, O. F. Mohammed, *ACS Cent. Sci.* 2023, **9**, 668. (b) H. M. Almushaikeh, H. Wang, L. Gutierrez-Arzaluz, J. Yin, R.-W. Huang, O. M. Bakr, O. F. Mohammed, *Chem. Commun.* 2023, **59**, 4447.
7. W. Zhao, Y. Wang, Y. Guo, Y. Suh, X. Liu, *Adv. Sci.*, 2023**, 10**, e2205526.
8. A. Vogler, H. Kunkely, *J. Am. Chem. Soc.* 1986, **108**, 7211.
9. K. R. Kyle, C. K. Ryu, J. A. DiBenedetto, P. C. Ford, P. C. *J. Am. Chem. Soc*. 1991, **113**, 2954.
10. S. Kondo, N. Yoshimura, M. Yoshida, A. Kobayashi, M. Kato, *Dalton* 2020**, 49**, 16946.
11. C.-H. Lam, W. K. Tang, V. W.-W. Yam, *Inorg. Chem.* 2023**, 62**,1942.
12. P. C. Ford, E. Cariati, J. L. Bourassa, *Chem. Rev.* 1999*,* **99,** 3625.
13. E. Cariati, E. Lucenti, C. Botta, U. Giovanella, D. Marinotto, S. Righetto, *Coord. Chem. Rev.* 2016, **306**, 566-614.
14. A. Nurtaeva, E. M. Holt, *Acta Cryst*. 1999, **C55**, 1453
15. J. Huang, B. Su, E. Song, M. S. Molokeev, Z. Xia, *Chem. Mater.* 2021, **33**, 4382.
16. S. Li, J. Xu, Z. Li, Z. Zeng, W. Li, M. Cui, C. C. Qin, Y. Du, *Chem. Mater*. 2020, **32**, 6525.
17. E. Jalilian, R. Z. Liao, F. Himo, H. Brismar, F. Laurelld, S. Lidine, *Cryst. Eng. Comm*, 2011, **13**, 4729.
18. M. Vitale, W. E. Palke, P. C. Ford, *J. Phys. Chem*., 1992, **96***,* 8329.
19. F. De Angelis, S. Fantacci, A. Sgamellotti, E. Cariati, R. Ugo, P. C. Ford, *Inorg. Chem.* 2006*,* **45***,* 1057.
20. M. J. Weber, *Nuclear Instruments and Methods in Physics Research A* 2004, **527**, 9.
21. (a) J. B. Birks, *Chem. Phys. Let*. 1970, **7**, 293-295. (b) J. Zhang, J. Li, X. Li, S. Yuan, Y. Sun, Y. Zou, Y. Pan, K. Zhang, *J. Mater. Chem. C*, 2022, **10**, 4795.
22. (a) L. Bergmann, G. J. Hedley, T. Baumann, S. Bräse, I. D. W. Samuel, *Sci. Adv.* 2016; **2**, e1500889. (b) R. W. Jones, A. J. Auty, G. Wu, P. Persson, M. V. Appleby, D. Chekulaev, C. R. Rice, J. A. Weinstein, P. I. P. Elliott, P. A. Scattergood, *J. Am. Chem. Soc*. 2023, **145**, 12081.
23. V. Geppert-Kleinrath, M. S. Freeman, C. R. Hurlbut, F. Merrill, J. R. Tinsley, P. Volegov, C. Wilde, *Rev. Sci. Instr* 2018, **89**, 10I142
24. M. Hunyadi, G. F. Samu, L. Csige, A. Csík, C. Buga, C. Janáky, *Adv. Funct. Mater.* 2022**, 32**, 2206645
25. K. Seki, T. Miura, T. Ikoma, *J. Phys. Chem. C* 2023, **127**, 9562